

## Ethylene Polymerization Activity of $(R_3P)Ni(codH)^+$ ( $cod = 1,5$ -cylcooctadiene) Sites Supported on Sulfated Zirconium Oxide

Jessica Rodriguez and Matthew P. Conley\*



Cite This: <https://doi.org/10.1021/acs.inorgchem.1c00454>



Read Online

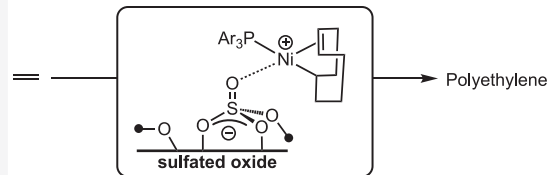
ACCESS |

Metrics & More

Article Recommendations

Supporting Information

**ABSTRACT:**  $PAR_3$  containing *o*-OMe, *o*-Me, or *o*-Et substituents reacts with Brønsted sites on sulfated zirconium oxide (SZO) to form  $[HPAR_3][SZO]$ . The phosphonium sites on this material react with bis(cyclooctadiene)nickel  $[Ni(cod)_2]$  to form  $[Ni(PAR_3)(codH)][SZO]$  that are active in ethylene polymerization reactions. Selective poisoning studies with pyridine show that  $\sim 90\%$  of the  $[Ni(PAR_3)(codH)]^+$  sites in this material are active in polymerization reactions.



### INTRODUCTION

Organometallic complexes of nickel and palladium containing the *o*-phosphinoarenesulfonate ligand ( $\{PO\}$ ) catalyze polymerization of olefins. In contrast to  $(\alpha$ -diimine)Pd-R $^+$  catalysts,<sup>1</sup>  $\{PO\}$ Pd-R complexes polymerize ethylene to form linear polymers<sup>2</sup> and show broad functional group tolerance in copolymerization reactions with polar comonomers.<sup>3</sup> The formation of linear polymers with  $\{PO\}$ Pd-R complexes is related to the *cis* arrangement of a strong-trans-influence phosphine and a weak-trans-influence sulfonate that results in electronic asymmetry in the palladium complex,<sup>4</sup> which inhibits  $\beta$ -H elimination and reinsertion steps that result in branches in the polymer chain.<sup>5</sup> This general design strategy continues to find application in new cationic palladium and nickel catalysts that incorporate electronically dissymmetric ligands and have very high polymerization activities and good functional group tolerance.<sup>6</sup>

Industrial olefin polymerization catalysts are almost always heterogeneous.<sup>7</sup> Silica pretreated with alkylaluminum or methaluminoxane (MAO) is a very common support for polymerization catalysts but is not generally compatible with late-transition-metal polymerization precatalysts. For example,  $(\alpha$ -diimine)Ni catalysts supported on MAO/SiO<sub>2</sub> have low polymerization activities, but modified  $(\alpha$ -diimine)NiBr<sub>2</sub> complexes containing hydroxyl groups react with SiO<sub>2</sub>/MAO and polymerize ethylene in the presence of an Et<sub>3</sub>Al<sub>2</sub>Cl<sub>3</sub> activator to give polymers with broad molecular weight distributions.<sup>8</sup>

Formation of well-defined organometallics on oxide surfaces is a potentially attractive synthetic strategy to access active sites for polymerization reactions.<sup>9</sup> In this reaction, a partially dehydroxylated oxide containing  $-OH$  groups on the surface reacts with an organometallic to form covalent M-O<sub>x</sub> ( $O_x =$  surface oxygen) or an electrophilic M--O<sub>x</sub> ion pair. Supports containing  $-OH$  groups with weak Brønsted acidity (e.g., SiO<sub>2</sub>) form M-O<sub>x</sub> and are inactive in polymerization reactions in the absence of exogenous activators.<sup>10</sup> However, M--O<sub>x</sub> ion

pairs form on supports containing  $-OH$  sites more Brønsted acidic than silica, such as sulfated oxides<sup>11</sup> or Lewis-acid-activated silica.<sup>12</sup> The reaction of  $(\alpha$ -diimine)NiMe<sub>2</sub> or  $(\alpha$ -diimine)PdMe<sub>2</sub> with sulfated zirconium oxide partially dehydroxylated at 300 °C (SZO<sub>300</sub>) forms the active sites shown in Figure 1a that have activities close to those of their solution analogues and show single-site behavior.<sup>13</sup>

The application of this strategy to surface analogues of  $\{PO\}M-R$  ( $M = Ni, Pd$ ) is not as straightforward.<sup>14</sup>  $\{PO\}$ PdR(L) are expected to react with  $-OH$  sites on oxides to form  $\{PO\}ML[SZO_{300}]$  ion pairs that lack the organometallic unit that is critical to propagate polymer growth (Figure 1b). Early reports of polymerization reactions with  $\{PO\}$ Pd complexes were generated from the reactions of Pd<sub>2</sub>dba<sub>3</sub> or Pd(OAc)<sub>2</sub> and  $\{PO\}H$ , which presumably forms  $\{PO\}$ Pd-H under the reaction conditions (Figure 2).<sup>15</sup> The Brønsted sites on SZO<sub>300</sub> react with sufficiently basic R<sub>3</sub>P to form  $[R_3PH][SZO_{300}]$ ,<sup>16</sup> which may serve as heterogeneous  $\{PO\}H$ -type surface sites. This paper describes the reaction of  $[R_3PH][SZO_{300}]$  with bis(cyclooctadiene)nickel  $[Ni(cod)_2]$  to produce active sites for the polymerization of ethylene.

### RESULTS AND DISCUSSION

This study focuses on Ar<sub>3</sub>P containing two aryl fragments with *ortho* substituents that are common in typical  $\{PO\}M-R$  catalysts. The reaction of triarylphosphines with the Brønsted sites on SZO<sub>300</sub> is expected to form  $[Ar_3PH][SZO_{300}]$ , provided that the  $pK_a$  value of  $[Ar_3PH]$  is greater than  $\sim 6$  in acetonitrile (MeCN).<sup>16</sup> For example,  $P(o\text{-OMeC}_6H_4)_2Ph$

**Special Issue:** Heterogeneous Interfaces through the Lens of Inorganic Chemistry

**Received:** February 13, 2021

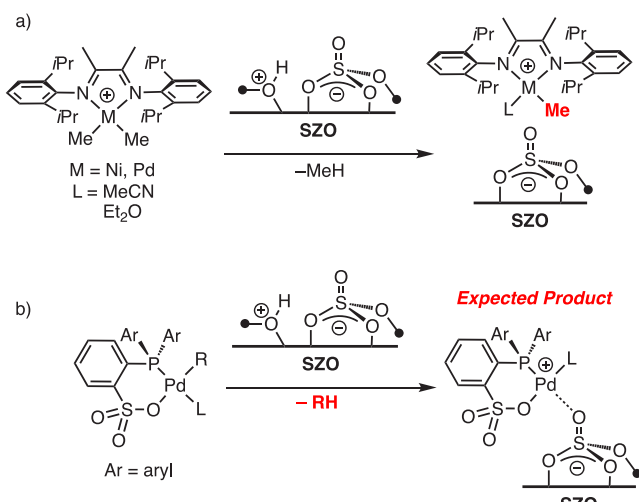


**Figure 1.** Heterogeneous ( $\alpha$ -diimine)Ni or -Pd catalysts supported on  $\text{SZO}_{300}$  for the polymerization of olefins (a). Related reaction of a  $\{\text{PO}\}\text{Pd}-\text{R}$  catalyst with  $\text{SZO}_{300}$  to form  $[\{\text{PO}\}\text{Pd}][\text{SZO}_{300}]$ , which are unreactive toward olefins (b).

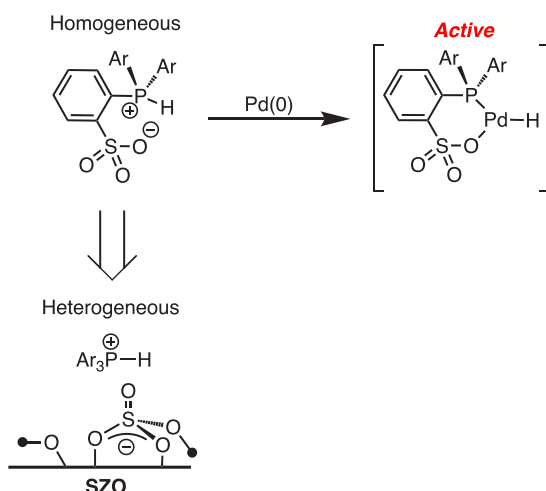


**Figure 2.** Reaction of  $\{\text{PO}\}\text{H}$  with  $\text{Pd}(0)$  to form  $\text{Pd}-\text{H}$  that is active in olefin polymerization in solution and design of  $[\text{HPAr}_3][\text{SZO}_{300}]$  to form heterogeneous  $\{\text{PO}\}\text{M}-\text{R}$  active sites.

reacts with  $\text{SZO}_{300}$  to form  $[\text{HP}(\text{o-OMeC}_6\text{H}_4)_2\text{Ph}][\text{SZO}_{300}]$  (1; Figure 3a). The  $^{31}\text{P}$  magic-angle-spinning (MAS) NMR spectrum of 1 contains a signal at 10 ppm (Figure 3b, top spectrum). The Fourier transform infrared (FTIR) spectrum of 1 is shown in Figure 3c (top) and contains a characteristic  $\nu_{\text{PH}}$  stretch at  $2456\text{ cm}^{-1}$ , consistent with formation of the phosphonium in  $[\text{1H}][\text{SZO}_{300}]$ . Similar results were obtained for reactions of  $\text{P}(\text{o-MeC}_6\text{H}_4)_2\text{Ph}$  or  $\text{P}(\text{o-EtC}_6\text{H}_4)_2\text{Ph}$  with  $\text{SZO}_{300}$  to form  $[\text{HP}(\text{o-MeC}_6\text{H}_4)_2\text{Ph}][\text{SZO}_{300}]$  ( $[2\text{H}][\text{SZO}_{300}]$ ) or  $[\text{HP}(\text{o-EtC}_6\text{H}_4)_2\text{Ph}][\text{SZO}_{300}]$  ( $[3\text{H}][\text{SZO}_{300}]$ ), respectively.

1–3 react with a clear yellow solution of  $\text{Ni}(\text{cod})_2$  in diethyl ether ( $\text{Et}_2\text{O}$ ) to form orange  $[\text{Ni}(\text{PAr}_3)(\text{codH})][\text{SZO}_{300}]$  (1Ni–3Ni; Figure 3a). This reaction also evolves 1,5-cyclooctadiene ( $0.10\text{ mmol g}^{-1}$ ), which is consistent with the loss of one cod per Ni in 1Ni–3Ni. Figure 3b (bottom) shows the FTIR spectrum of 1Ni, which lacks a  $\nu_{\text{PH}}$  stretch. In addition, the  $^{31}\text{P}$  MAS NMR spectrum of 1Ni contains a new signal at 47 ppm, 37 ppm downfield from that of 1. These

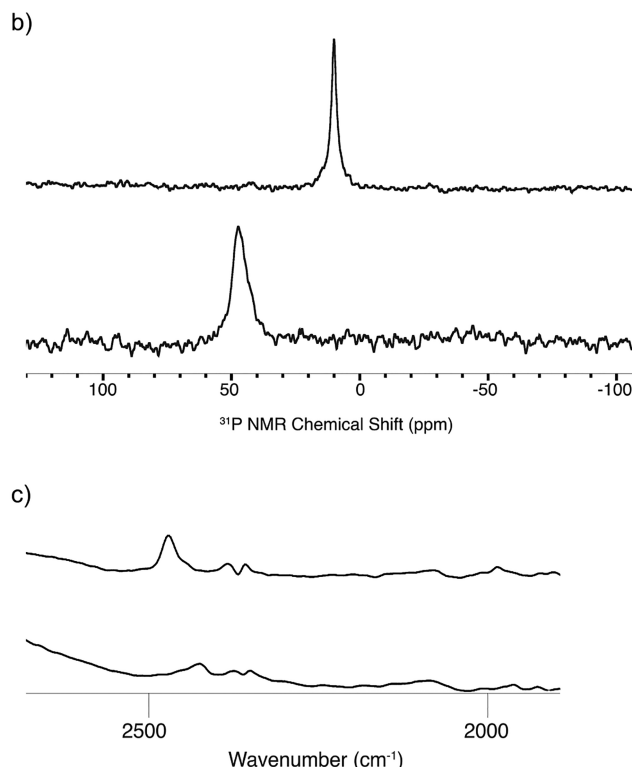
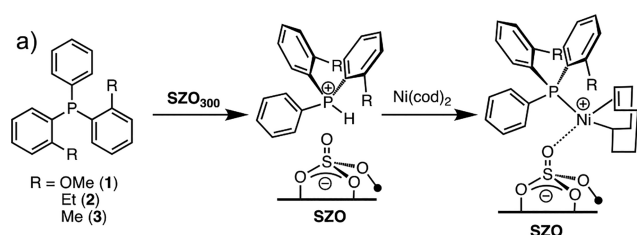


**Figure 3.** Formation of  $[\text{Ni}(\text{PAr}_3)(\text{codH})][\text{SZO}]$  (a).  $^{31}\text{P}^{[1\text{H}]}$  MAS NMR spectrum of 1 (top) and  $[\text{Ni}(\text{P}(\text{o-OMeC}_6\text{H}_4)_2\text{Ph})(\text{codH})][\text{SZO}_{300}]$  (bottom, b). FTIR of 1 (top) and  $[\text{Ni}(\text{P}(\text{o-OMeC}_6\text{H}_4)_2\text{Ph})(\text{codH})][\text{SZO}_{300}]$  (bottom, c).

results indicate that the phosphonium in 1 reacts with  $\text{Ni}(\text{cod})_2$  to form 1Ni. The cross-polarization  $^{13}\text{C}$  MAS NMR spectra of 1Ni–3Ni contain signals assigned to the  $(\text{codH})^+$  fragment in  $\text{Ni}(\text{PAr}_3)(\text{codH})^+$ .<sup>17</sup> The key NMR and FTIR features of 1 and 1Ni are summarized in Table 1.

1Ni reacts with 150 psi of ethylene on demand at  $50\text{ }^\circ\text{C}$ , which results in the formation of polyethylene containing 35 branches/1000C (Table 2, entry 1).  $^{13}\text{C}$  NMR analysis of the polymer shows that methyl, ethyl, and butyl branches are present in this polymer. Contacting 1Ni with a slight excess of

**Table 1.** Key Spectral Data for  $[\text{HPAr}_3][\text{SZO}_{300}]$  and  $[\text{Ni}(\text{PAr}_3)(\text{codH})][\text{SZO}_{300}]$

$\text{PAr}_3$	$[\text{HPAr}_3][\text{SZO}_{300}]$		$[\text{Ni}(\text{PAr}_3)(\text{codH})]$	
	$\delta^{31}\text{P}$ (ppm) <sup>a</sup>	$\delta^{31}\text{P}$ (ppm) <sup>b</sup>	$\nu_{\text{PH}}$ ( $\text{cm}^{-1}$ )	$\delta^{31}\text{P}$ (ppm) <sup>b</sup>
1	−26.4	10	2456	47
2	−22.4	13	2447	45
3	−20.8	11	2454	45

<sup>a</sup> $\text{C}_6\text{D}_6$  solution, referenced to 85%  $\text{H}_3\text{PO}_4$ . <sup>b</sup>10 kHz MAS spinning speed, referenced to 85%  $\text{H}_3\text{PO}_4$ .

**Table 2. Ethylene Polymerization Activity of  $[\text{Ni}(\text{PAr}_3)(\text{codH})][\text{SZO}_{300}]$ <sup>a</sup>**

entry	PAr <sub>3</sub>	P (psi) <sup>b</sup>	T (°C)	yield (mg)	activity <sup>c</sup>	B/1000C <sup>d</sup>
1	1	150	50	71	3000(150)	35
2	2	150	50	82	3400(100)	20
3	3	100	50	12	510(10)	n.d.
4	3	150	50	83	3500(100)	24
5	3	200	50	91	3500(500)	n.d.
6	3	250	65	80	3400(300)	n.d.

<sup>a</sup>Catalyst loading (12 μmol) in toluene (see the Supporting Information for details). <sup>b</sup>Pressure of ethylene on demand. <sup>c</sup>g<sub>PE</sub> mol<sub>Ni</sub><sup>-1</sup> h<sup>-1</sup> calculated from triplicate polymerization runs assuming that all Ni in  $[\text{Ni}(\text{PAr}_3)(\text{codH})][\text{SZO}_{300}]$  is active in polymerization. The values in parentheses are the associated standard errors based on the polymer yield. <sup>d</sup>Measured by <sup>1</sup>H NMR spectroscopy in CD<sub>2</sub>Cl<sub>4</sub> at 120 °C.

pyridine (Ni:pyridine = 1:1.2) results in complete suppression of the polymerization activity, indicating that pyridine poisons Ni sites in the polymerization reaction. The addition of substiochiometric pyridine to **1Ni** followed by reaction with 150 psi of ethylene on demand results in the formation of polyethylene, although with a lower activity than that of reactions conducted in the absence of pyridine. Plots of the activity versus the molar ratio of pyridine to Ni are linear and indicate that ~90% of the Ni sites in **1Ni** are capable of initiating ethylene polymerization (Figure S8).

The polymerization activity data for **1Ni**–**3Ni** are given in Table 2. The activity of **1Ni** under these conditions is 3000(150) g<sub>PE</sub> mol<sub>Ni</sub><sup>-1</sup> h<sup>-1</sup>. This activity is modest compared to that of {PO}M–R species but similar to that of catalysts prepared from {PO}H with similar steric profiles and Pd(0) sources *in situ*.<sup>18</sup> **2Ni** (Table 2, entry 2) and **3Ni** (Table 2, entry 4) show similar activities and similar branching of the polyethylene produced with these catalysts. Running polymerization reactions at lower pressures with **3Ni** results in lower polymerization activity (Table 2, entry 3), but higher pressures do not result in significant activity gains (Table 2, entries 5 and 6). The formation of branched polymer products using **1Ni**–**3Ni** is in contrast to polymers obtained with homogeneous {PO}Pd–R or {PO}Ni–R catalysts in solution. The origin of this difference is unclear but may be related to the formation of a weakly coordinating ion pair between  $\text{Ni}(\text{PAr}_3)(\text{codH})^+$  and the sulfate sites on  $\text{SZO}_{300}$ ,<sup>11</sup> which may facilitate chain walking.

**1Ni**–**3Ni** are not compatible with allyl chloride or methyl undecenoate, suggesting that further optimization of the Ni sites in these catalysts is needed to accommodate functionalized olefins. Attempts to analyze the polymers by gel permeation chromatography to obtain molecular weight information were unsuccessful because of the low solubility of the polymer in 1,2,4-trichlorobenzene at 140 °C and complications in removing  $\text{SZO}$  from these solutions.<sup>19</sup>

## CONCLUSIONS

Triarylphosphines react with  $\text{SZO}_{300}$  to form  $[\text{HPAr}_3][\text{SZO}_{300}]$ . Subsequent reactions of the phosphonium sites with  $\text{Ni}(\text{cod})_2$  to form  $[\text{Ni}(\text{PAr}_3)(\text{codH})][\text{SZO}_{300}]$  are active in the polymerization of ethylene to give polymers with moderate branching in the polymer chain. The activity of  $[\text{Ni}(\text{PAr}_3)(\text{codH})][\text{SZO}_{300}]$  in polymerization is modest but similar to that of first-generation {PO}Pd catalysts. This

suggests that modification of the coordination environment of the  $\text{Ni}(\text{codH})^+$  site by tuning the sterics and electronics of the phosphine may result in more active catalysts or catalysts tolerant of olefins containing functional groups.

## ASSOCIATED CONTENT

### Supporting Information

The Supporting Information is available free of charge at <https://pubs.acs.org/doi/10.1021/acs.inorgchem.1c00454>.

Experimental details, solid-state NMR spectra, SEM images, and FTIR data (PDF)

## AUTHOR INFORMATION

### Corresponding Author

Matthew P. Conley – Department of Chemistry, University of California—Riverside (UCR), Riverside, California 92521, United States;  [orcid.org/0000-0001-8593-5814](https://orcid.org/0000-0001-8593-5814); Email: [matthew.conley@ucr.edu](mailto:matthew.conley@ucr.edu)

### Author

Jessica Rodriguez – Department of Chemistry, University of California—Riverside (UCR), Riverside, California 92521, United States

Complete contact information is available at:

<https://pubs.acs.org/10.1021/acs.inorgchem.1c00454>

### Notes

The authors declare no competing financial interest.

## ACKNOWLEDGMENTS

M.P.C. is a member of the UCR Center for Catalysis. This work was supported by the National Science Foundation (Grant CHE-1800561).

## REFERENCES

- (a) Ittel, S. D.; Johnson, L. K.; Brookhart, M. Late-Metal Catalysts for Ethylene Homo- and Copolymerization. *Chem. Rev.* **2000**, *100*, 1169–1204. (b) Muhammad, Q.; Tan, C.; Chen, C. Concerted steric and electronic effects on  $\alpha$ -diimine nickel- and palladium-catalyzed ethylene polymerization and copolymerization. *Science Bulletin* **2020**, *65*, 300–307.
- (a) Nakamura, A.; Anselment, T. M. J.; Claverie, J.; Goodall, B.; Jordan, R. F.; Mecking, S.; Rieger, B.; Sen, A.; van Leeuwen, P. W. N.; Nozaki, K. Ortho-Phosphinobenzenesulfonate: A Superb Ligand for Palladium-Catalyzed Coordination-Insertion Copolymerization of Polar Vinyl Monomers. *Acc. Chem. Res.* **2013**, *46*, 1438–1449. (b) Chen, C. Designing catalysts for olefin polymerization and copolymerization: beyond electronic and steric tuning. *Nat. Rev. Chem.* **2018**, *2*, 6–14.
- (a) Tan, C.; Chen, C. Emerging Palladium and Nickel Catalysts for Copolymerization of Olefins with Polar Monomers. *Angew. Chem., Int. Ed.* **2019**, *58*, 7192–7200. (b) Nakamura, A.; Ito, S.; Nozaki, K. Coordination-Insertion Copolymerization of Fundamental Polar Monomers. *Chem. Rev.* **2009**, *109*, 5215–5244.
- Conley, M. P.; Jordan, R. F. *Cis/trans* Isomerization of Phosphinesulfonate Palladium(II) Complexes. *Angew. Chem., Int. Ed.* **2011**, *50*, 3744–3746.
- Nakano, R.; Chung, L. W.; Watanabe, Y.; Okuno, Y.; Okumura, Y.; Ito, S.; Morokuma, K.; Nozaki, K. Elucidating the Key Role of Phosphine–Sulfonate Ligands in Palladium-Catalyzed Ethylene Polymerization: Effect of Ligand Structure on the Molecular Weight and Linearity of Polyethylene. *ACS Catal.* **2016**, *6*, 6101–6113.
- (a) Zhang, W.; Waddell, P. M.; Tiedemann, M. A.; Padilla, C. E.; Mei, J.; Chen, L.; Carrow, B. P. Electron-Rich Metal Cations Enable Synthesis of High Molecular Weight, Linear Functional Polyethylenes.

*J. Am. Chem. Soc.* **2018**, *140*, 8841–8850. (b) Liang, T.; Goudari, S. B.; Chen, C. A simple and versatile nickel platform for the generation of branched high molecular weight polyolefins. *Nat. Commun.* **2020**, *11*, 372.

(7) (a) Severn, J. R.; Chadwick, J. C.; Duchateau, R.; Friederichs, N. "Bound but Not Gagged" Immobilizing Single-Site  $\text{CE}\pm$ -Olefin Polymerization Catalysts. *Chem. Rev.* **2005**, *105*, 4073–4147. (b) Hlatky, G. G. Heterogeneous Single-Site Catalysts for Olefin Polymerization. *Chem. Rev.* **2000**, *100*, 1347–1376.

(8) (a) Preishuber-Pflugl, P.; Brookhart, M. Highly Active Supported Nickel Diimine Catalysts for Polymerization of Ethylene. *Macromolecules* **2002**, *35*, 6074–6076. (b) Schrekker, H. S.; Kotov, V.; Preishuber-Pflugl, P.; White, P.; Brookhart, M. Efficient Slurry-Phase Homopolymerization of Ethylene to Branched Polyethylenes Using a Diimine Nickel(II) Catalysts Covalently Linked to Silica Supports. *Macromolecules* **2006**, *39*, 6341–6354.

(9) (a) Copéret, C.; Chabanas, M.; Petroff Saint-Arroman, R.; Basset, J.-M. Homogeneous and Heterogeneous Catalysis: Bridging the Gap through Surface Organometallic Chemistry. *Angew. Chem., Int. Ed.* **2003**, *42*, 156–181. (b) Marks, T. J. Surface-bound metal hydrocarbols. Organometallic connections between heterogeneous and homogeneous catalysis. *Acc. Chem. Res.* **1992**, *25*, 57–65. (c) Wegener, S. L.; Marks, T. J.; Stair, P. C. Design Strategies for the Molecular Level Synthesis of Supported Catalysts. *Acc. Chem. Res.* **2012**, *45*, 206–214. (d) Stalzer, M.; Delferro, M.; Marks, T. Supported Single-Site Organometallic Catalysts for the Synthesis of High-Performance Polyolefins. *Catal. Lett.* **2015**, *145*, 3–14. (e) Copéret, C.; Comas-Vives, A.; Conley, M. P.; Estes, D. P.; Fedorov, A.; Mougel, V.; Nagae, H.; Núñez-Zarur, F.; Zhizhko, P. A. Surface Organometallic and Coordination Chemistry toward Single-Site Heterogeneous Catalysts: Strategies, Methods, Structures, and Activities. *Chem. Rev.* **2016**, *116*, 323–421.

(10) (a) Dorcier, A.; Merle, N.; Taoufik, M.; Bayard, F.; Lucas, C.; de Mallmann, A.; Basset, J. M. Preparation of a Well-Defined Silica-Supported Nickel-Diimine Alkyl Complex Application for the Gas-Phase Polymerization of Ethylene. *Organometallics* **2009**, *28*, 2173–2178. (b) Popoff, N.; Gauvin, R. M.; De Mallmann, A.; Taoufik, M. On the Fate of Silica-Supported Half-Metallocene Cations: Elucidating a Catalyst's Deactivation Pathways. *Organometallics* **2012**, *31*, 4763–4768.

(11) Witzke, R. J.; Chapovetsky, A.; Conley, M. P.; Kaphan, D. M.; Delferro, M. Non-Traditional Catalyst Supports in Surface Organometallic Chemistry. *ACS Catal.* **2020**, *10*, 11822–11840.

(12) (a) Culver, D. B.; Venkatesh, A.; Huynh, W.; Rossini, A. J.; Conley, M. P.  $\text{Al}(\text{ORF})_3$  ( $\text{RF} = \text{C}(\text{CF}_3)_3$ ) activated silica: a well-defined weakly coordinating surface anion. *Chem. Sci.* **2020**, *11*, 1510–1517. (b) Walzer, J. F. Supported Ionic Catalyst Composition. U.S. Patent 5,643,847. (c) Millot, N.; Santini, C. C.; Baudouin, A.; Basset, J.-M. Supported cationic complexes: selective preparation and characterization of the well-defined electrophilic metallocenium cation  $\text{SiO-B(C}_6\text{F}_5)_3\text{}-[\text{Cp}^*\text{ZrMe}_2(\text{Et}_2\text{NPh})]^+$  supported on silica. *Chem. Commun.* **2003**, 2034–2035.

(13) (a) Culver, D. B.; Tafazolian, H.; Conley, M. P. A Bulky Pd(II)  $\alpha$ -Diimine Catalyst Supported on Sulfated Zirconia for the Polymerization of Ethylene and Copolymerization of Ethylene and Methyl Acrylate. *Organometallics* **2018**, *37*, 1001–1006. (b) Tafazolian, H.; Culver, D. B.; Conley, M. P. A Well-Defined Ni(II)  $\alpha$ -Diimine Catalyst Supported on Sulfated Zirconia for Polymerization Catalysis. *Organometallics* **2017**, *36*, 2385–2388.

(14) For heterogeneous polymerization using dispersed molecular  $\{\text{PO}\}\text{Pd-R}$  complexes, see: Dai, S.; Chen, C. A Self-Supporting Strategy for Gas-Phase and Slurry-Phase Ethylene Polymerization using Late-Transition-Metal Catalysts. *Angew. Chem., Int. Ed.* **2020**, *59*, 14884–14890. For  $\{\text{PO}\}\text{Pd-R}$  sites immobilized on polystyrene, see: Wucher, P.; Schwaderer, J. B.; Mecking, S. Solid-Supported Single-Component Pd(II) Catalysts for Polar Monomer Insertion Copolymerization. *ACS Catal.* **2014**, *4*, 2672–2679.

(15) (a) Drent, E.; van Dijk, R.; van Ginkel, R.; van Oort, B.; Pugh, R. I. Palladium catalysed copolymerisation of ethene with alkylacrylates: polar comonomer built into the linear polymer chain. *Chem. Commun.* **2002**, 744–745. (b) Drent, E.; van Dijk, R.; van Ginkel, R.; van Oort, B.; Pugh, R. I. The first example of palladium catalysed non-perfectly alternating copolymerisation of ethene and carbon monoxide. *Chem. Commun.* **2002**, 964–965.

(16) Rodriguez, J.; Culver, D. B.; Conley, M. P. Generation of Phosphonium Sites on Sulfated Zirconium Oxide: Relationship to Brønsted Acid Strength of Surface – OH Sites. *J. Am. Chem. Soc.* **2019**, *141*, 1484–1488.

(17) Peuckert, M.; Keim, W. A new nickel complex for the oligomerization of ethylene. *Organometallics* **1983**, *2*, 594–597.

(18) Vela, J.; Lief, G. R.; Shen, Z.; Jordan, R. F. Ethylene Polymerization by Palladium Alkyl Complexes Containing Bis(aryl)-phosphino-toluenesulfonate Ligands. *Organometallics* **2007**, *26*, 6624–6635.

(19) Similar observations were noted in polyethylene synthesized using electrophilic organozirconium sites supported on SZO and attributed to the formation of ultrahigh-molecular-weight products. See: Nicholas, C. P.; Ahn, H.; Marks, T. J. Synthesis, Spectroscopy, and Catalytic Properties of Cationic Organozirconium Adsorbates on Super Acidic Sulfated Alumina. Single-Site Heterogeneous Catalysts with Virtually 100 % Active Sites. *J. Am. Chem. Soc.* **2003**, *125*, 4325–4331.